Published in final edited form as:
Proteins. 2015 February ; 83(2): 383–388. doi:10.1002/prot.24705.

Structure of a Cupin Protein Plu4264 from *Photorhabdus luminescens* subsp. laumondii TTO1 at 1.35 Å Resolution

R. Sophia Weerth[1], **Karolina Michalska**[2,3], **Craig A. Bingman**[4], **Ragothaman M. Yennamalli**[5], **Hui Li**[3], **Robert Jedrzejczak**[3], **Fengbin Wang**[5], **Gyorgy Babnigg**[2,3], **Andrzej Joachimiak**[2,3], **Michael G. Thomas**[1], and **George N. Phillips Jr.**[5,$]

[1]Department of Bacteriology, University of Wisconsin-Madison, Madison, Wisconsin, USA

[2]Midwest Center for Structural Genomics, Biosciences Division, Argonne National Laboratory, Argonne, Illinois,, USA

[3]Structural Biology Center, Biosciences Division, Argonne National Laboratory, Argonne, Illinois, USA

[4]Department of Biochemistry, University of Wisconsin-Madison, Madison, Wisconsin, USA

[5]Biosciences at Rice, Rice University, Houston, Texas, USA

Abstract

Proteins belonging to the cupin superfamily have a wide range of catalytic and non-catalytic functions. Cupin proteins commonly have the capacity to bind a metal ion with the metal frequently determining the function of the protein. We have been investigating the function of homologous cupin proteins that are conserved in more than 40 species of bacteria. To gain insights into the potential function of these proteins we have solved the structure of Plu4264 from *Photorhabdus luminescens* TTO1 at a resolution of 1.35 Å and identified manganese as the likely natural metal ligand of the protein.

Keywords

Cupin; X-ray; Structural Genomics; Natural Product; Manganese-bound

Introduction

The cupin protein superfamily was established to distinguish proteins by their distinctive β-barrel fold yet they possess diverse functionality.[1,2] To date, both catalytic and non-catalytic cupin proteins have been identified, such as sugar binding effector proteins, dioxygenases and decarboxylases. Cupin proteins are identified by their overall structure and through the presence of two conserved motifs $G(X)_5\mathbf{H}X\mathbf{H}(X)_{3,4}\mathbf{E}(X)_6G$ and $G(X)_5PXG(X)_2\mathbf{H}(X)_3N$, where the letters in bold represent the residues that can be responsible for metal binding. In some cases one of the two histidinyl residues in motif 1 can be replaced by glutaminyl,

[$]Corresponding Author: George N. Phillips, Jr, Biosciences at Rice, Rice University, 6100 Main St., Houston, Texas, 77005, USA, georgep@rice.edu.

aspartyl or glutamyl residues.[1] Currently, the range of metals known to be coordinated by these four residues are cadmium, cobalt, copper, iron, manganese, nickel and zinc.[1,2] The function of a cupin protein is frequently dictated by the bound metal. For example, cupin dioxygenases bind to iron or nickel, while the cupin decarboxylases are manganese dependent. Interestingly, there are cases where these residues do not bind metal, rather they are involved in positioning the substrate in the active site as observed for some sugar isomerases.[2]

We have been interested in a group of putative cupin proteins that we identified using a bioinformatics approach to natural product discovery. The genes coding for these cupin homologs are always associated with two other genes that code for a methionyl-tRNA synthetase (MetRS) homolog and a lysine/ornithine N-hydroxylase homolog in more than 40 bacterial species. Interestingly, in some species the cupin is fused to the N-terminus of the MetRS homolog, suggesting a coordinated function between these enzymes. These gene clusters have been noticed by others,[3,4] but neither a metabolite nor a function has been associated with them yet. To aid in deciphering the function of these gene clusters in these various bacterial species, we took a structural genomics approach. A crystal screen using several cupin proteins encoded by the targeted gene clusters identified conditions for the crystallization of Plu4264, a 14.5 KDa protein of unknown function from *Photorhabdus luminiscens* subsp. laumondii TTO1. Here we present the structure of this protein at 1.35 Å resolution, provide evidence that the natural metal ligand is manganese, and discuss the implications of the structure on the potential substrate for this enzyme.

Results and Discussion

Protein purification, crystallization and structure elucidation was performed by the Midwest Center for Structural Genomics. The crystal structure of Plu4264 was determined using SAD phasing to a resolution of 1.35 Å. Detailed data collection and refinement statistics are presented in Table 1. Two molecules of Plu4264 are present in the asymmetric unit, forming a homodimer. The final structure consists of amino acids from Se-Met2 through Asp122 for each protein monomer, with no electron density observed for the C-terminal His_6-tag (residues 123-128). Two ions of Ni^{2+}, one Na^{+}, and 288 water molecules are present in the asymmetric unit. All residues are in the favored regions of the Ramachandran plot generated by MolProbity.[5]

Each monomer of Plu4264 comprises of 120 amino acids that form 11 β-strands, forming two antiparallel β-sheets, one α-helix, with one monomer having a small helix 3_{10} (η1, in monomer A only). The two β-sheets form the jellyroll β-sandwich (Figure 1A) that is indicative of a cupin β-barrel fold. The homodimer is formed by having the first β-strand (β1) of each monomer (residues 1-6) crossover to its neighboring monomer and form part of the β-sheet with strand β9 of the opposite monomer (Figure 1, Supplementary Figure S1). Additionally, the C-terminal end of each Plu4264 monomer forms an amphipathic α-helix (Asp109-Glu121). The hydrophobic interface that is formed between the two helices consists of Leu113, Leu116 and Leu119 and the carbon side-chain of Lys109 (the amino group is oriented away from the interface). The antiparallel α-helices are at approximately 20° angle to one another, allowing for the hydrophobic ridge and groove formation between

the two helices. Sequence alignments and secondary structure prediction suggest that the amphipathic helices are present in the majority of the putative cupins we identified, suggesting that the helices may be specific to the function of these proteins. Finally, there is a large hydrophobic interface between the β-barrels of each monomer, forming a surface area of approximately 1900 $Å^2$ (calculated using PISA[6]) that creates the main interactions between the two monomers.

Plu4264 has the two characteristic motifs of cupin proteins that include the residues that form the nickel-binding site (Figure 1B). Interestingly, several flexible loop regions (residues 46-55, 68-75, and 84-92) close to the metal were observed from analysis of the backbone residues B-factors and the real-space correlation coefficient (Supplementary Figure S2). To further investigate the loop flexibility, we ran a Phenix ensemble refinement on the structure[7,8] (Figure 1C). The ensemble refinement results validate the proposed loop flexibility, reduce the R/R_{free}, and increase the overall map correlation coefficient (F-model vs 2*m*Fo-*d*Fc). Details of the ensemble refinement were included in the supplemental documents (Supplementary Table S1), and the corresponding coordinates were deposited in the Protein Data Bank (PDB) (4Q29). Several DALI-based close structural homologs of cupin were also analyzed on those loop regions: they all have some similar loop flexibilities, but not necessarily in all the three regions (Supplementary Figure S3).

The electron density of the crystal structure reveals Ni^{2+} coordinated by His50, His52, His90, and Glu56, it is reasonable to propose that this Ni^{2+} may be a product of the purification scheme, which included Ni^{2+}-affinity chromatography. To investigate this metal-binding capacity in more detail, we cloned the gene encoding Plu4264 into pTYB2, resulting in a fusion protein with C-terminal self-cleaving chitin binding domain. The protein lacking the affinity tag was purified to near homogeneity based on SDS-PAGE analysis. We used differential scanning fluorimetry (DSF)[9] to determine the likely metal ligand *in vivo*. The DSF analysis showed an 8°C increase in thermostability of Plu4264 when manganese was added, compared to the metal free control (Supplementary Figure S4). All other metals (iron, nickel, zinc, copper, and cobalt) significantly decreased thermostability of Plu4264, with the exception of magnesium, which had no impact on the thermostablity. The increased thermostability of Plu4264 in the presence of only manganese suggests that it is the functionally relevant metal. Analysis of the His-tagged protein used for crystallization also determined that only manganese increased the thermostability of the protein, providing additional support for the conclusion that manganese is the functionally relevant metal.

The DALI server and 3D-Blast showed a close structural relationship between Plu4264 and Tm1287 (PDB entry 1O4T, Dali Z-score=13.7, 3D-Blast score=108), a structure of a putative oxalate decarboxylase homodimer.[10] Tm1287 was crystallized with oxalate and manganese in the binding pocket. Due to the size difference and the lack of the C-terminal α-helices in the Tm1287 structure, the full structures could not be well aligned structurally. A structural alignment (residues 35-107 of Plu4264 and 46-119 of Tm1287) showed clear homology between the β-barrel folds (Figure 2A). The structural alignment used 257 atoms out of the selection and gave an RMS of 0.9 Å. The Tm1287 structure shows both motifs encompassed within two pairs of β-strands, which is typical for cupins. In the case of

Plu4264 the fifth β-strand does not extend far enough to encompass the first half of motif 1. However, the side chain arrangement suggests a suboptimal assignment by the DSSP algorithm, as it appears the β-strand should stretch from Thr45 to His52. The structural alignment of Tm1287 with Plu4264 supports this hypothesis, as the fifth β-strand of Tm1287 aligns with the backbone of Thr45 to His52 from Plu4264 (Figure 2A).

Although the barrel alignment sets the metal binding sites in similar conformations, the non-conserved regions between the two motifs show two very different substrate binding pockets. The Plu4264 binding pocket shows a cavity more than twice as large as and more hydrophobic than Tm1287 (537.8 $Å^3$ vs. 210.8 $Å^3$, respectively; calculated by CASTp[11] (Figure 2B)). Additionally, the mouths of the cavities reflect the differences in the size of the cavities themselves, where Plu4624 cavity mouth is 59.9 $Å^2$ and the Tm1287 cavity mouth is 24.8 $Å^2$. The size difference of both the cavities and their entry point suggest that Plu4264 accepts a substrate that is significantly larger than that of Tm1287, which has putatively been assigned as oxalate. In addition, the functionality of Tm1287 is far removed from the predicted functionality of Pfam 07883 assigned to Plu4264 through NCBI, which mostly encompasses sugar-binding isomerases. Taking into consideration the substrate binding pocket parameters and manganese being the functional metal, the function of Plu4264 could be akin to that of Tm1287 but with a larger, less charged substrate.

Materials and Methods

Gene cloning

The gene cloning was performed according to Y. Kim *et al.*[12] *P. luminescens* subsp. laumondii TTO1 genomic DNA was used as a template for PCR with the following primers in the reaction mixture:
5′GGAGTAAAGATAATGATGAATATTATTCGTAAAATGGATTGGGATTCAAT and 5′GTGATGGTGATGATGATCCTGCTCTAATCGGGTAAGAAAGTTC. The purified PCR product was treated with T4 polymerase in the presence of dGTP according to vendor specification (New England Biolabs, Ipswich, Massachusetts, USA). The protruded DNA fragment was mixed with the LIC-ready vector pMCSG81 (http://mcsg.anl.gov/) according to the ligation-independent cloning procedure[13] and transformed to the *E. coli* BL21(DE3) Gold cells. The pMCSG81 vector introduces C-terminal non-cleavable His_6-tag with no extra amino acids besides the hexahistidine fragment. A single colony was picked, grown and induced with isopropyl-β-D-thiogalactoside (IPTG). The cell lysate was analyzed for presence of the protein with the right molecular weight. The solubility was analyzed via small scale Ni^{2+} affinity purification.

Protein expression, purification and crystallization

The starter cultures were grown at 37°C overnight in 500 mL polyethylene terephthalate bottles containing 25 mL of non-sterile modified M9 salts “pink” medium.[14] It was then transferred to a 2 L polyethylene terephthalate bottle containing 1 L of M9 “pink” media with 100 μg/ml ampicillin. Cells were allowed to grow at 37°C, and shaken at 200 rpm until OD_{600} reached 1.4. They were cooled down to 18° C before inhibitory amino acids (150 mg each of L-valine, L-isoleucine, L-leucine, L-lysine, L-threonine, L-phenylalanine), 90 mg

selenomethionine (Medicilon, Inc., Shanghai, China, catalog number MD045004D), and 1 mM IPTG were added to the culture. Cells were then grown overnight at 18°C, and harvested the next morning. 7 g of cells were resuspended in 30 ml of lysis buffer containing 50 mM HEPES pH 8.0, 500 mM NaCl, 5% (v/v) glycerol, 10 mM imidazole, and 10 mM β-mercaptoethanol, plus 1 protease inhibitor cocktail tablet (cOmplete ULTRA, Roche, Branford, CT, USA). Resuspended cells were stored in -80° C refrigerator before processing.

Frozen cells were thawed and lysed on ice for 30 minutes. Lysate was sonicated for 5 minutes and centrifuged at 30,000 g for 60 minutes followed by filtration through 0.45 μm syringe filters. Clarified lysates were loaded on ÄKTAxpress system (GE Healthcare Life Sciences, Piscataway, NJ, USA) for automated purification using Ni^{2+} affinity chromatography followed by size exclusion chromatography on the HiLoad 26/60, Superdex 200 column (GE Healthcare Life Sciences). A single peak was collected from the size exclusion chromatography column. Protein was then concentrated and buffer-exchanged with Amicon Ultra filters (Millipore, Bedford, MA, USA) to crystallization buffer containing 20 mM HEPES pH 8.0, 250 mM NaCl, and 2 mM dithiothreitol (DTT).

Protein at concentration of 50 mg/ml was used to set up crystallization using Mosquito liquid dispenser (TTP Labtech, Cambridge, MA, USA). MCSG1, MCSG2, MCSG3, and MCSG4 crystallization screens (Microlytic, Woburn, MA, USA) were used for the screening through vapor diffusion technique. 500 nl of protein was mixed with 500 nl of each crystallization reagent and was allowed to equilibrate at 16°C in 96-well CrystalQuick sitting-drop plates (Greiner Bio-one, Monroe, NC, USA). X-ray quality crystals appear from several conditions, and the best dataset was collected from MCSG4 E3 condition containing 0.2 M Li_2SO4, 0.1 M Tris/HCl, pH 8.5, 25% (v/v) PEG400.

Data collection

Prior to data collection, the Se-labeled protein crystals were flash-cooled in liquid nitrogen without additional cryoprotection. The X-ray diffraction experiment was carried out at the Structural Biology Center beamline 19-ID at the Advanced Photon Source, Argonne National Laboratory. The single-wavelength anomalous diffraction (SAD) dataset was collected at 100K near the selenium K-absorption edge. The diffraction images were processed with the HKL3000 suite.[15] Intensities were converted to structure factor amplitudes in the Ctruncate program from the CCP4 package.[16] The data collection and refinement statistics are given in Table 1.

Structure solution and refinement

The structure was solved by the SAD method using selenium peak data and the HKL3000 software pipeline.[15] Positions of heavy atoms were determined in SHELXD and initial phases were obtained from SHELXE.[17] The heavy atom sites were refined and improved phases were calculated by iterations of MLPHARE[16] and DM.[17] The initial protein model was built in ARP/wARP.[18] The final model was obtained through alternating manual rebuilding in COOT[19] and crystallographic refinement in Phenix.[20] The structure was refined with anisotropic B factors for all atoms. The refinement statistics is shown in Table

1. The atomic coordinates and structure factors have been deposited in the PDB under accession code 4MV2.

Cloning of Plu4264 with chitin binding domain

The Plu4264 gene was cloned into the multiple cloning site region of pTYB2 (New England Biolabs [NEB]). Genomic DNA of *P. luminescens* subsp. laumondii TTO1 was isolated using Wizard® Genomic DNA Purification Kit (Promega, Madison, WI, USA). The gene was amplified using the following primers: 5′-AAGGAGATATACATATGATGAATATTATTCGTAAAATGGA-3′ (N-term) and 5′-CTTGGCAAAGCACCCGGGATCCTGCTCTAATCGGG-3′ (C-term). pTYB2 was cut using restriction enzymes *Sma*I and *Nde*I (NEB) using the recommended buffers. The amplified Plu4264 was ligated into the open vector using T4 DNA ligase (NEB). Ligation products were transformed into *E. coli* DH5α, and plated on Lysongeny Broth (LB) plates containing ampicillin (100 μg/mL). All potential clones had their plasmids isolated using Wizard® Miniprep Kit (Promega). Plasmids were checked for inserts using double restriction digest (*Sma*I and *Nde*I), and analyzed using gel electrophoresis. Plasmids containing the Plu4264 insert were transformed into *E. coli* BL21 (DE3).

On-column cleavage and purification of Plu4264

For the starter culture, *E. coli* BL21(DE3) transformants, carrying Plu4264+pTYB2 plasmid, were inoculated into 50 mL LB media (10 g/L tryptone, 5 g/L yeast extract, 10 g/L NaCl) in 250 ml flasks, and incubated overnight at 37°C. Three 2 L beveled Fernbach flasks, each containing 1 L LB media, were inoculated with 15 mL starter culture each. The cultures were shaken at 200 rpm at 28°C until OD_{600} of 0.6 was reached. Cultures were induced with a final concentration of 100 μM IPTG and temperature was shifted to 15°C. The remaining purification methods follow instructions of the NEB IMPACT™ T7 protocol. Flasks remained shaking overnight. Cultures were centrifuged at 7,000 rpm for 30 minutes. The pellet was resuspended in 2.5 × its weight of lysis buffer (20 mM Na-HEPES pH 8.0, 500 mM NaCl, 0.1 mM EDTA, 0.1% Triton X-100). To lyse the cells the suspension was sonicated at 30% for 15 minutes with 1 second pulses. The lysed cells were centrifuged at 15,000 rpm for 30 minutes. During centrifugation a column containing 6 mL chitin beads (NEB) was equilibrated with 60 mL lysis buffer. The cell extract, containing the protein, was loaded onto the column. The column was washed with 100 mL lysis buffer (at a flow rate no faster than 0.5 ml/min). For on column cleavage the column was quickly flushed with 18 mL cleavage buffer (20 mM HEPES pH 8.0, 50 mM NaCl, 0.1 mM EDTA) containing 30 mM DTT. The flow of the column was stopped, leaving the beads suspended in cleavage buffer, and incubated at 4°C overnight. The protein was eluted using 18 mL cleavage buffer (no DTT added), and flow through was collected in 3 mL-fractions. Fractions were analyzed using 15% SDS-PAGE gel to confirm presence of Plu4264. Fractions 4-6 were pooled and concentrated to 1.74 mg/mL using Centriprep YM-3 centrifugal filters (Millipore).

Differential Scanning Fluorimetry

The DSF assays were performed in a BioRad MyIQ™ Real Time PCR cycler, and data were recorded by the BioRad MyIQ™ software (BioRad, Hercules, CA, USA). The machine was calibrated following the hand book guidelines provided by BioRad. Calibrations were performed biweekly during the assay period. Assays were run using a Cy™ 3/ VIC™ /HEX/TET filter with 575/20 nm excitation. The reactions were run in 96-well PCR plates and covered by plastic film (BioRad), with 25 μL reaction volume per well. The final reaction conditions were 500 μM metal ($FeSO_4$, ferric citrate, $MnCl_2$, $NiCl_2$, $ZnSO_4$, $CuSO_4$ or $Co(NO_3)_2$), 70 μM Plu4264, 15× SYPRO® Orange Dye (Invitrogen) and buffer (starting concentration of 20 mM HEPES pH 8, 50 mM NaCl). The MyIQ™ protocol was run with 60 minutes incubation at 4°C for metal exchange, with subsequent temperature increase of 1°C with 10 second dwell times, until final temperature of 95°C. Fluorimetry data were exported and analyzed in Microsoft Excel.

Sequence alignments and secondary structure prediction

All sequence alignments were performed using the muscle alignment function of the MegAlign-Pro Program from the DNAstar Lasergene® 11 Core Suite. The sequences that aligned with the C-terminal α-helix (Asp109 – Glu121) from Plu4264 were entered into the Lasergene Protean Program for secondary structure prediction. Amphipathic α-helices were predicted through the Eisenberg method[24].

Supplementary Material

Refer to Web version on PubMed Central for supplementary material.

Acknowledgments

This work was supported by National Institutes of Health grants GM098248 (GP), GM094585 (AJ) and the U. S. Department of Energy, Office of Biological and Environmental Research, under contract DE-AC02-06CH11357 (AJ).

References

1. Dunwell JM, Purvis A, Khuri S. Cupins: the most functionally diverse protein superfamily? Phytochemistry. 2004; 65:7–17. [PubMed: 14697267]
2. Agarwal G, Rajavel M, Gopal B, et al. Structure-based phylogeny as a diagnostic for functional characterization of proteins with a cupin fold. PLoS One. 2009; 4:e5736. [PubMed: 19478949]
3. Aravind L, de Souza RF, Iyer LM. Predicted class-I aminoacyl tRNA synthetase-like proteins in non-ribosomal peptide synthesis. Biol Direct. 2010; 5:48. [PubMed: 20678224]
4. Iyer LM, Abhiman S, de Souza RF, et al. Origin and evolution of peptide-modifying dioxygenases and identification of the wybutosine hydroxylase/hydroperoxidase. Nucleic Acids Res. 2010; 38:5261–5279. [PubMed: 20423905]
5. Chen VB, Arendall WB, Headd JJ, et al. MolProbity: all-atom structure validation for macromolecular crystallography. Acta Crystallogr D Biol Crystallogr. 2010; 66:12–21. [PubMed: 20057044]
6. Krissinel E, Henrick K. Inference of macromolecular assemblies from crystalline state. J Mol Biol. 2007; 372:774–797. [PubMed: 17681537]
7. Levin EJ, Kondrashov DA, Wesenberg GE, et al. Ensemble refinement of protein crystal structures: validation and application. Structure. 2007; 15:1040–1052. [PubMed: 17850744]

8. Burnley BT, Afonine PV, Adams PD, et al. Modelling dynamics in protein crystal structures by ensemble refinement. Elife. 2012; 1:e00311. [PubMed: 23251785]
9. Cummings MD, Farnum MA, Nelen MI. Universal screening methods and applications of ThermoFluor. J Biomol Screen. 2006; 11:854–863. [PubMed: 16943390]
10. Schwarzenbacher R, von Delft F, Jaroszewski L, et al. Crystal structure of a putative oxalate decarboxylase (TM1287) from *Thermotoga maritima* at 1.95 Å resolution. Proteins. 2004; 56:392–395. [PubMed: 15211523]
11. Binkowski TA. CASTp: Computed Atlas of Surface Topography of proteins. Nucleic Acids Res. 2003; 31:3352–3355. [PubMed: 12824325]
12. Kim Y, Babnigg G, Jedrzejczak R, et al. High-throughput protein purification and quality assessment for crystallization. Methods. 2011; 55:12–28. [PubMed: 21907284]
13. Eschenfeldt WH, Lucy S, Millard CS, et al. A family of LIC vectors for high-throughput cloning and purification of proteins. Methods Mol Biol. 2009; 498:105–115. [PubMed: 18988021]
14. Donnelly MI, Zhou M, Millard CS, et al. An expression vector tailored for large-scale, high-throughput purification of recombinant proteins. Protein Expr Purif. 2006; 47:446–454. [PubMed: 16497515]
15. Minor W, Cymborowski M, Otwinowski Z, et al. HKL-3000: the integration of data reduction and structure solution--from diffraction images to an initial model in minutes. Acta Crystallogr D Biol Crystallogr. 2006; 62:859–866. [PubMed: 16855301]
16. Winn MD, Ballard CC, Cowtan KD, et al. Overview of the CCP4 suite and current developments. Acta Crystallogr D Biol Crystallogr. 2011; 67:235–242. [PubMed: 21460441]
17. Sheldrick GM. A short history of SHELX. Acta Crystallogr A. 2008; 64:112–122. [PubMed: 18156677]
18. Otwinowski, Z. Maxiumum likelihood refinement of heavy atom parameters. In: Wolf, W.; Evans, PR.; Leslie, AGW., editors. Isomorphous Replacement and Anomalous Scattering: Proceedings of the CCP4 Study Weekend. Warrington, England: 1991. p. 80-86.
19. Emsley P, Cowtan K. Coot: model-building tools for molecular graphics. Acta Crystallogr D Biol Crystallogr. 2004; 60:2126–2132. [PubMed: 15572765]
20. Langer G, Cohen SX, Lamzin VS, et al. Automated macromolecular model building for X-ray crystallography using ARP/wARP version 7. Nat Protoc. 2008; 3:1171–1179. [PubMed: 18600222]

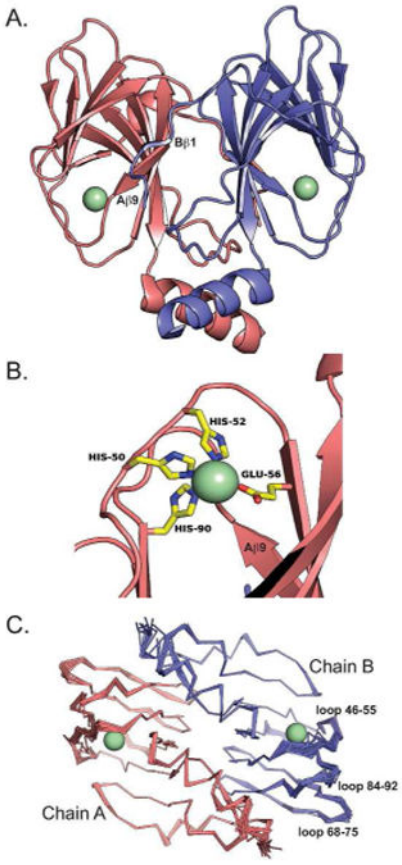

Figure 1. Crystal structure of Plu4264

(A) Cartoon representation of Plu4264, with Ni^{2+} ions represented as green spheres. Chain A is colored in red and chain B is colored blue. The β-strand from chain B (Bβ1) that crosses over to complex with Aβ9 of chain A to form part of the β-sheet for chain A is noted. A similar crossover is observed in chain B. (B) Cartoon representation of chain A Ni^{2+} coordination site with the responsible residues labeled and represented as sticks (carbon atoms are yellow, nitrogen atoms are blue and oxygen atoms are red, hydrogen atoms are not shown). Chain A is rotated approximately 180° relative to the orientation in Fig. 1A. (C) Loop flexibility of Plu4264. All conformations of the loops are represented as separate lines. The dimer is rotated approximately 90° north relative to the orientation in Fig. 1A.

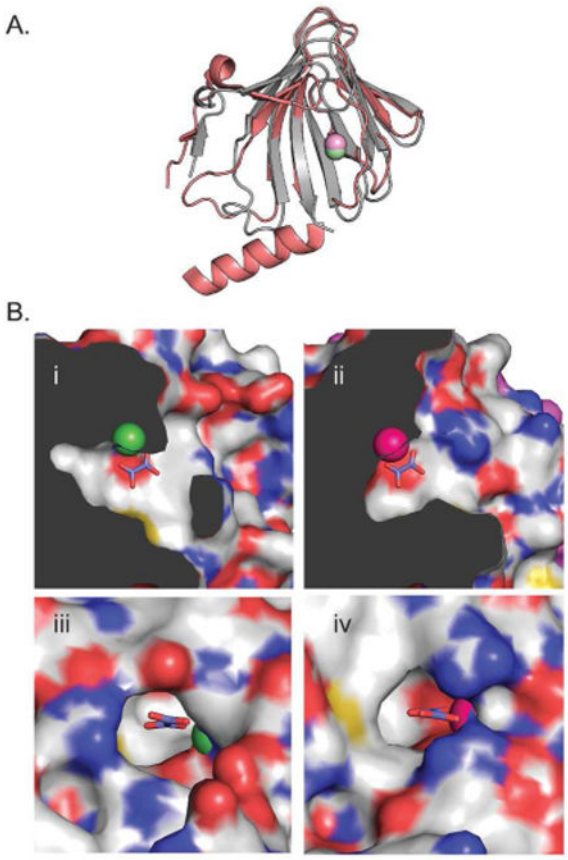

Figure 2. Structural alignment of Tm1287 with Plu4264

(A) Alignment of chain-A β-barrels of Plu4264 and Tm1287, shown as cartoon. Tm1287 is represented in pink along with the magnesium ion represented as a sphere in its binding pocket. Plu4264 is shown in blue, with the nickel ion represented as a green sphere. (B) Plu4264 and Tm1287 binding pockets are shown as surface representation. Panels Bi and Bii show a slice across the binding pocket of Plu4264 and Tm1287, respectively, with the grey area represents the protein interior. Panels Biii and Biv show the cavity entry sites of Plu4264 and Tm1287, respectively. Carbon atoms are colored white, oxygen atoms are colored red, nitrogen atoms are colored blue and sulfur atoms are colored yellow. The metal ions are represented as spheres in their respective binding pockets, where the nickel is colored green and the manganese is colored pink. The oxalate from the Tm1287 structure, represented as sticks, was shown in both binding pockets for size comparison.

Table 1

Data collection and refinement statistics

Data collection	
Space group	$C222_1$
Cell dimensions [Å]	a= 55.7 b=147.7 c=83.8
Temperature [K]	100
Radiation source	APS, 19-ID
Wavelength [Å]	0.97915
Resolution [Å][a]	30.00 – 1.35 (1.37 – 1.35)
Unique reflections	76,134 (3769)
R_{merge}[b]	0.084 (0.891)
Mean I/sigma(I)	26.8 (2.0)
Completeness [%]	99.8 (99.9)
Redundancy	7.1 (6.9)
Refinement	
Resolution [Å]	24.90 -1.35
Reflections work/test set	74,978/1113
R_{work} / R_{free}[c]	0.136/0.159
No. of atoms protein/ion/water	23,42/3/293
Average B factor [$Å^2$] protein/ion/water	19.5/16.6/31.3
RMSD from ideal	
bond lengths [Å]	0.013
bond angles [deg]	1.46
Ramachandran plot [%]	
favored	98.73
outliers	0
Molprobity score	1.25
Clashscore	3.71

[a] Values in parentheses correspond to the highest resolution shell.

[b] Rmerge = $\Sigma h \Sigma j |Ihj - \langle Ih \rangle| / \Sigma h \Sigma j Ihj$, where Ihj is the intensity of observation j of reflection h.

[c] $R = \Sigma h |Fo| - |Fc| / \Sigma h |Fo|$ for all reflections, where Fo and Fc are observed and calculated structure factors, respectively. Rfree is calculated analogously for the test reflections, randomly selected and excluded from the refinement.